

## Supplementary information

### DEER Experiments Reveal Fundamental Differences between Calmodulin Complexes with IQ and MARCKS Peptides in Solution

Chandrima Jash,<sup>1,#</sup> Akiva Feintuch,<sup>1,#</sup> Shira Naor,<sup>1</sup> Nurit Manukovsky,<sup>1</sup> Elwy H. Abdelkader,<sup>2</sup> Sudeshna Bhattacharya,<sup>1</sup> Gunnar Jeschke,<sup>3</sup> Gottfried Otting,<sup>2</sup> Daniella Goldfarb\*<sup>1</sup>

<sup>1</sup>Department of Chemical and Biological Physics, Weizmann Institute of Science, Rehovot Israel.<sup>2</sup> ARC Centre of Excellence for Innovations in Peptide & Protein Science, Research School of Chemistry, Australian National University, Canberra, ACT 2605, Australia.

<sup>3</sup>Laboratory of Physical Chemistry, ETH Zürich, Switzerland.

#### Contents

1. CaM mutants labelled with the C1 tag.....	S2
2. DEER data of holo-CaM-C1 with and without MARCKS .....	S2
3. Echo-detected EPR spectra.....	S5
4. EPR spectra of MA-proxyl-labelled CaM with and without peptides .....	S5
5. Primary DEER data of doubly labelled CaM.....	S6
6. DEER data on CaM dimerization .....	S7
7. EPR spectra of MTSL-labelled MARCKS with CaM.....	S8
8. Native gel .....	S9
9. Trilateration calculations of the location of the nitroxide label on the peptides .....	S10
10. Primary DEER data of singly labelled CaM with singly labelled peptides.....	S11
11. EPR spectra of MTSL-labelled IQ peptide with CaM.....	S12
12. Predicted vs experimental distance distributions in the CaM/IQ complex.....	S13
13. DEER data of doubly labelled IQ with CaM.....	S13
14. NMR data .....	S14
16. SDS gel .....	S19

## 1. CaM mutants labelled with the C1 tag

**Table S1.** CaM double cysteine mutants labelled with C1 tag

	N-domain labelling	C-domain labelling
	Position	Position
1	T34C-C1	A103C-C1
2	T34C-C1	T110C-C1
3	T34C-C1	E119C-C1
4	T44C-C1	A103C-C1
5	T44C-C1	T110C-C1
6	T44C-C1	E119C-C1
7	N53C-C1	A103C-C1
8	N53C-C1	T110C-C1
9	N53C-C1	E119C-C1

## 2. DEER data of holo-CaM-C1 with and without MARCKS

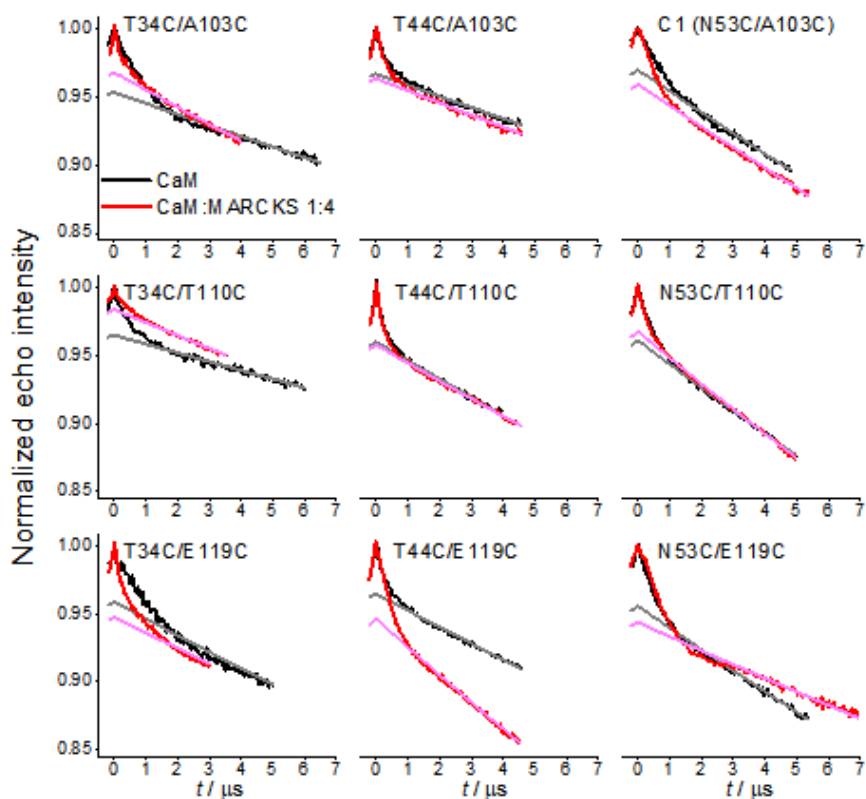


**Figure S1.** Primary DEER traces for nine CaM mutants in the absence (black traces) or presence (red lines) of MARCKS in 4-fold excess with the corresponding background decays in grey and pink.

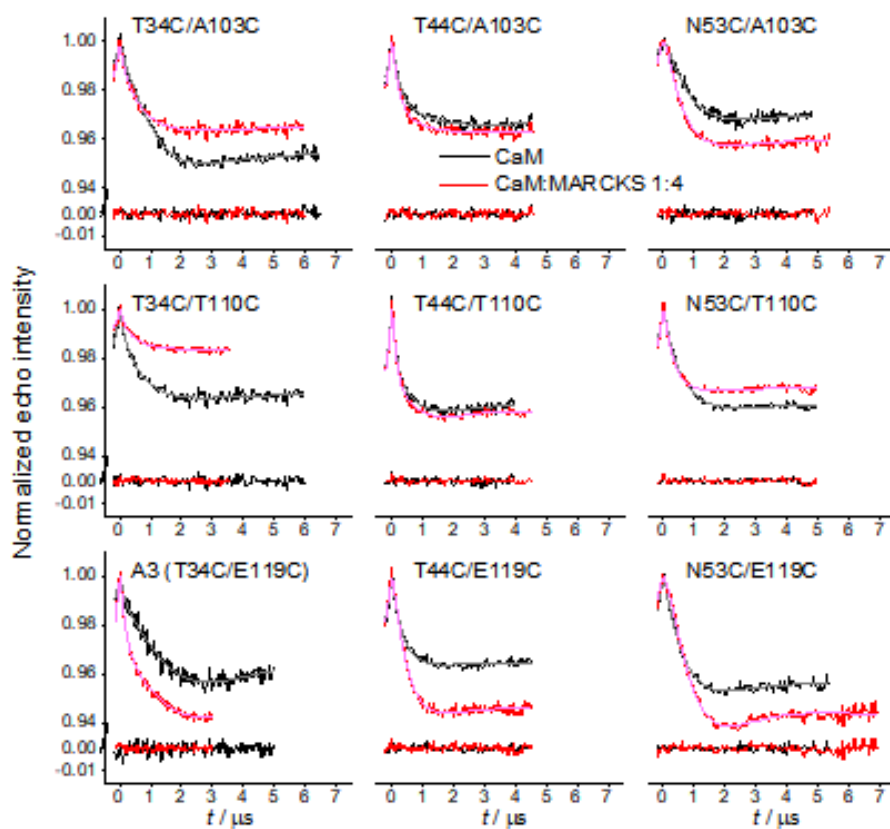


**Figure S2.** Background-corrected DEER traces for nine CaM mutants in the absence (black traces) or presence (red traces) of MARCKS peptide in 4-fold excess, including the two-Gaussian GLADD fits (grey and pink traces respectively) and their residuals.

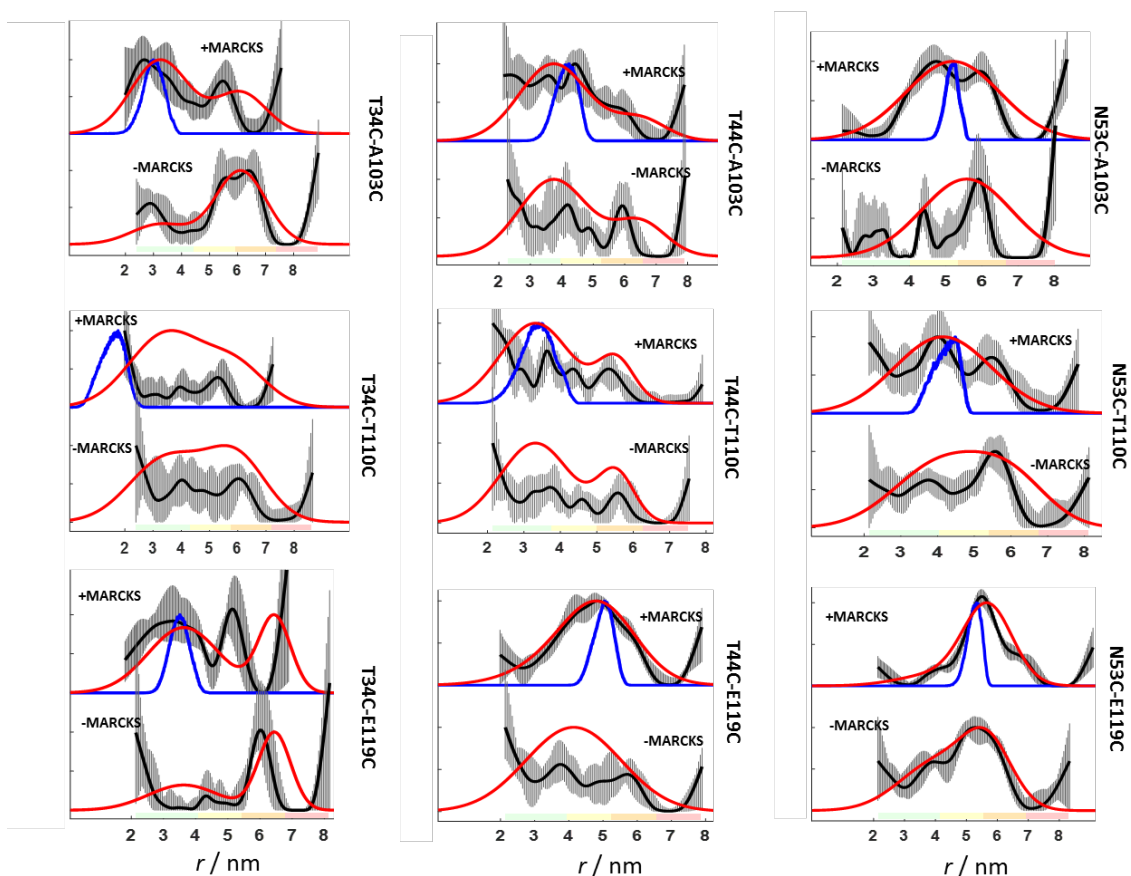


**Figure S3.** DEER distance distributions for nine CaM mutants in the absence (bottom traces) or presence (top traces) of MARCKS peptide in 4-fold excess, calculated using Tikhonov regularization as implemented in DeerAnalysis (black traces). The color bars indicate the reliability regions as defined in DeerAnalysis, depending on the DEER evolution time used (pale green: the shape of the distance distribution is reliable, pale yellow: the mean distance and distribution width are reliable; pale orange: the mean distance is reliable; pale red: long-range distance contributions may be detectable, but cannot be quantified.) The solid lines represent the distributions with the smallest r.m.s.d. from the experimental data and the striped regions represent the variation of alternative distributions ( $\pm 2$  times the standard deviation) obtained by varying the parameters of the background correction and noise as calculated by the validation tool in the DeerAnalysis software package with the default values. The red traces represent the fit obtained with GLADD global fit with two Gaussians for each mutant (red trace). The blue trace displays the distance distribution predicted from the crystal structure 1IWQ.

### 3. Echo-detected EPR spectra

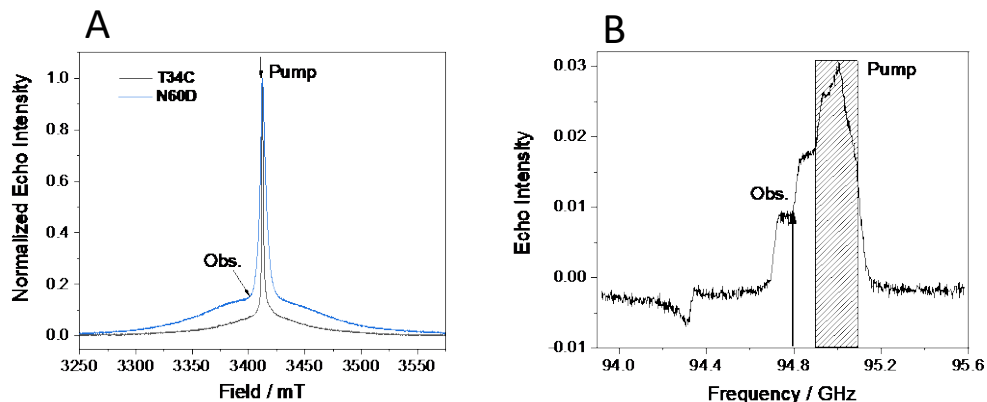


**Figure S4.** Echo-detected EPR spectra (10K) of singly-labelled CaM. (A) Representative echo-detected EPR spectra of CaM N60D-Gd(III) and CaM T34C-Gd(III)-DOTA-M. The ZFS is much higher in the case of the N60D-Gd(III) mutant. (B) Echo-detected EPR spectrum of the IQ peptide bound to singly-labelled CaM (T117) converted to a frequency axis. The pump (denoted by shaded region) and observe positions (denoted by arrows) used for Gd(III)–NO DEER experiments are identified.

### 4. EPR spectra of MA-proxyl-labelled CaM with and without peptides

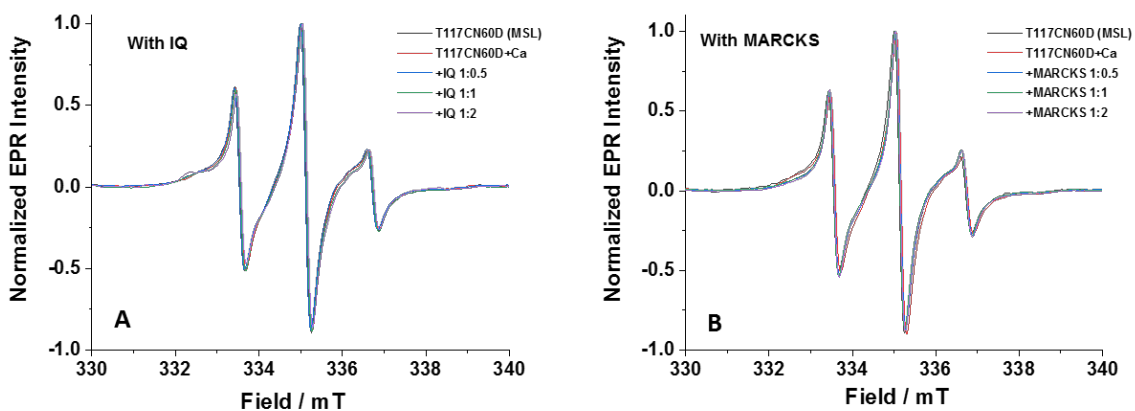


**Figure S5.** Room temperature X-band EPR spectra of CaM T117C-MA-proxyl without and with  $\text{Ca}^{2+}$  ions, in the presence of different concentrations of peptide. (A) With IQ peptide. (B) With MARCKS peptide.

## 5. Primary DEER data of doubly labelled CaM

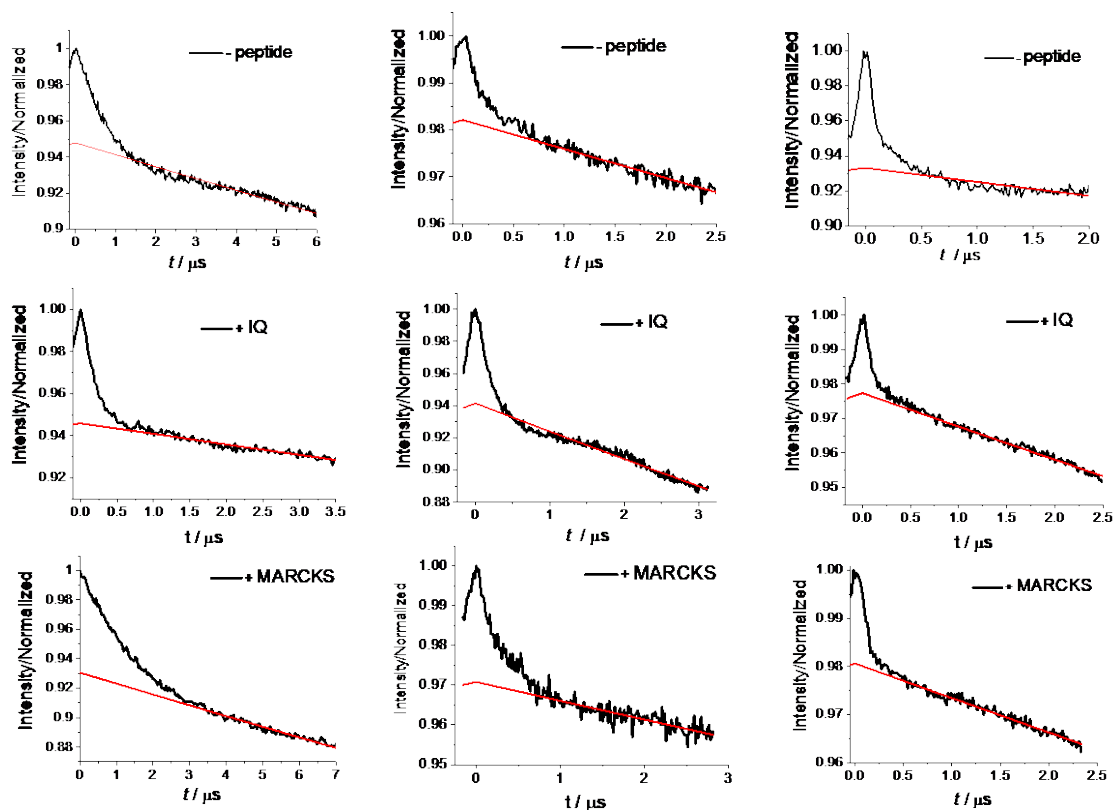


**Figure S6.** Primary DEER traces for three CaM double mutants in the absence or presence of peptides in 1:1 molar ratio. Column A shows the data for the mutant T117C/T34C, column B shows the data for N60D/T117C and column C shows the data for N60D/T34C.

## 6. DEER data on CaM dimerization

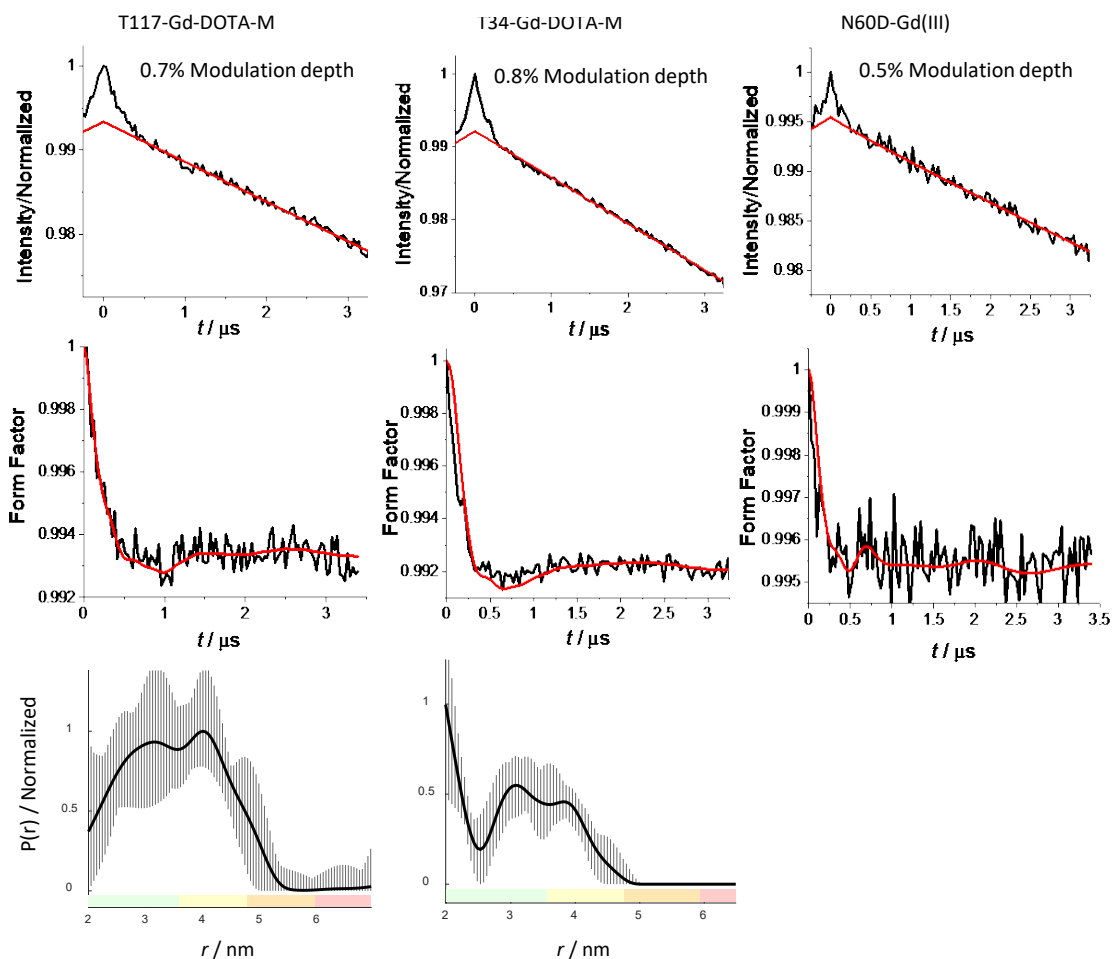


**Figure S7.** Primary and fitted DEER traces for the three CaM single mutants in the absence of peptides. Panels A–C show the Gd(III)–Gd(III) DEER data (black) for the constructs T117-Gd(III)-DOTA-M, T34-Gd(III)-DOTA-M and N60D-Gd(III). In the top row, red lines correspond to the background fit, in the middle row, they correspond to the Tikhonov regularization fit. The bottom row shows the corresponding distance distributions. The signal-to-noise ratio of the data of the N60D mutant was too low for analysis.

## 7. EPR spectra of MTSL-labelled MARCKS with CaM

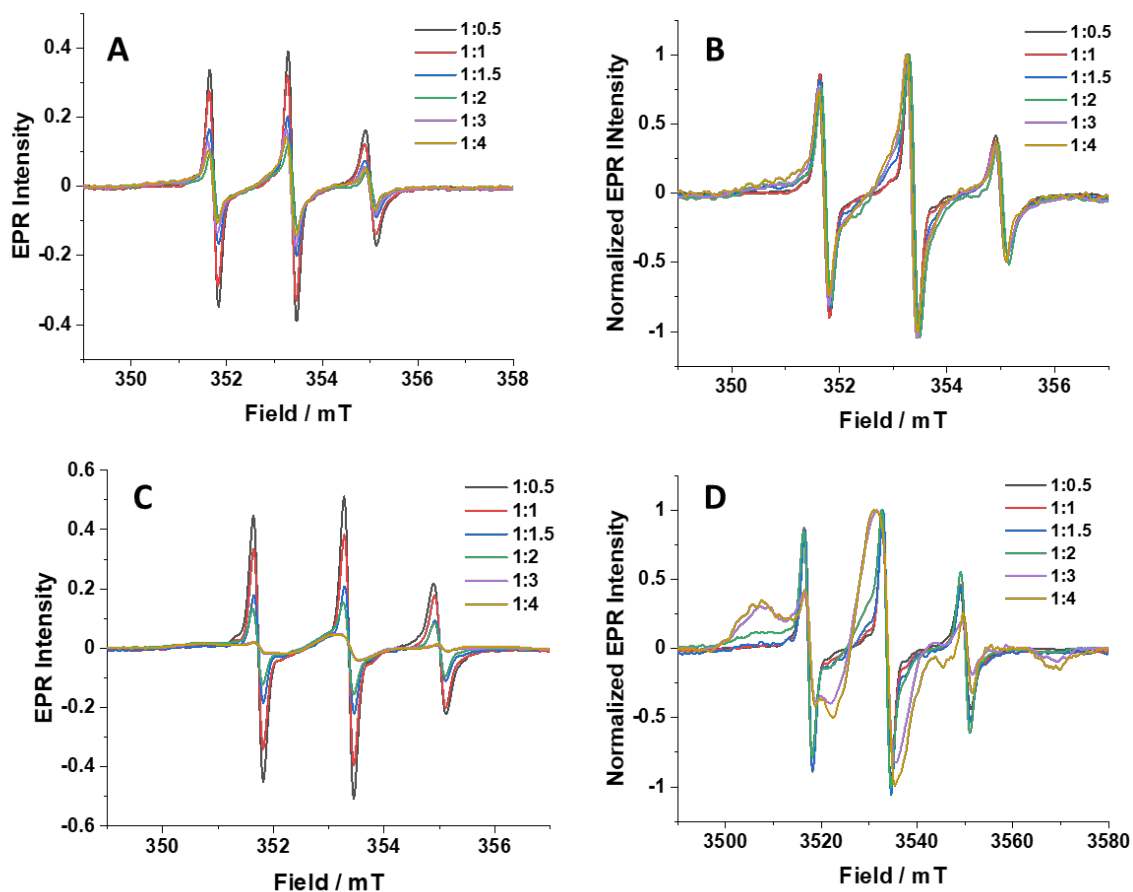


**Figure S8.** Room temperature X-band CW EPR measurements of MARCKS (50  $\mu$ M) binding to CaM. (A) Titration with increasing amounts of the CaM mutant T117C (molar ratios indicated in the figure) carried out in the absence of  $\text{Ca}^{2+}$  ions (with EDTA present). (B) Same as (A) but following normalization of the spectra to the same maximum intensity to facilitate comparison of the lineshapes. (C) and (D) Same as (A) and (B) but in the presence of 5 mM  $\text{Ca}^{2+}$  ions.

## 8. Native gel

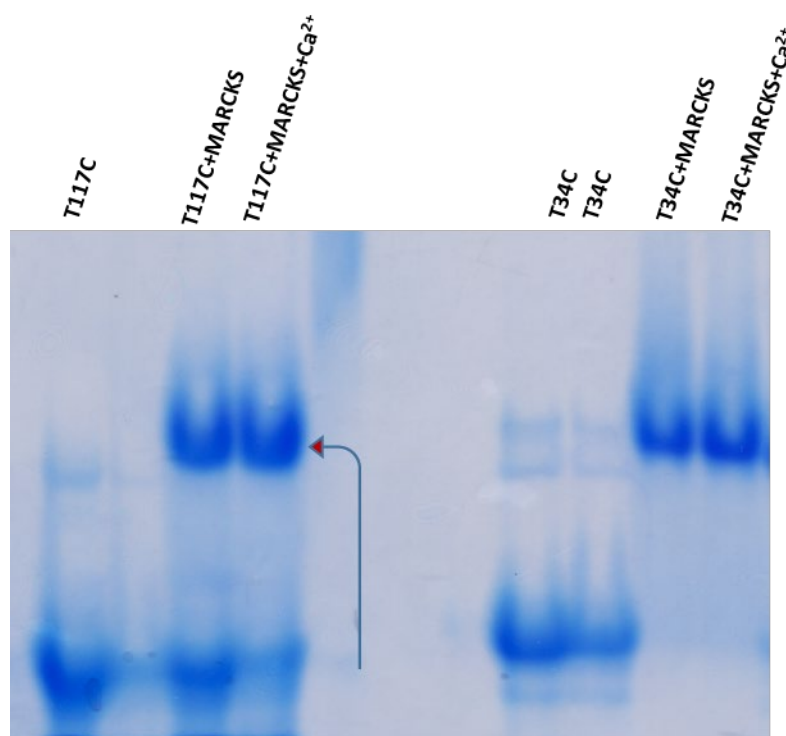


**Figure S9.** Native 12% PAGE of CaM T117C and T34C labelled with Gd-DOTA-M in the presence of MARCKS (with and without Ca<sup>2+</sup>). The protein:peptide ratio was 1:1 and the shift in the band position indicates the binding of peptide to the protein.

## 9. Trilateration calculations of the location of the nitroxide label on the peptides

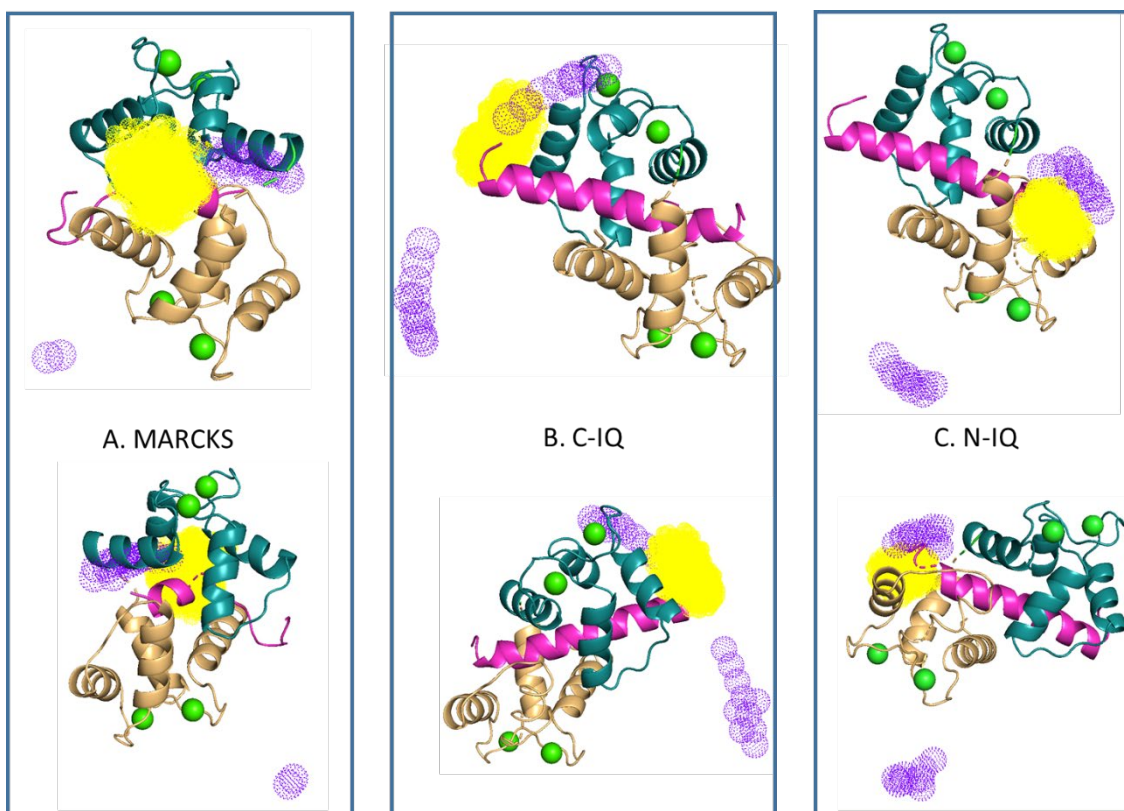


**Figure S10.** Results of the trilateration calculations for the NO radical group location (shown in purple) relative to the CaM structure using an ensemble calculation of 20 solutions. For comparison the predicted MTSL rotamer cloud is shown in yellow for (A.) MARCKS, (B.) C-IQ and (C.) N-IQ. For (B) and (C) the structure is of chain A. Note that with three distances between reference sites and the unknown site, a mirror-image ambiguity results in trilateration with respect to the plane defined by the reference label sites. Hence, for each construct, only one of the two purple clouds can be expected to overlap with the yellow cloud. For each case two different views are presented to highlight the degree of overlap between the predicted MTSL location (yellow cloud) and the one extracted by trilateration (purple balls), revealing the poorest overlap for MARCKS.

## 10. Primary DEER data of singly labelled CaM with singly labelled peptides

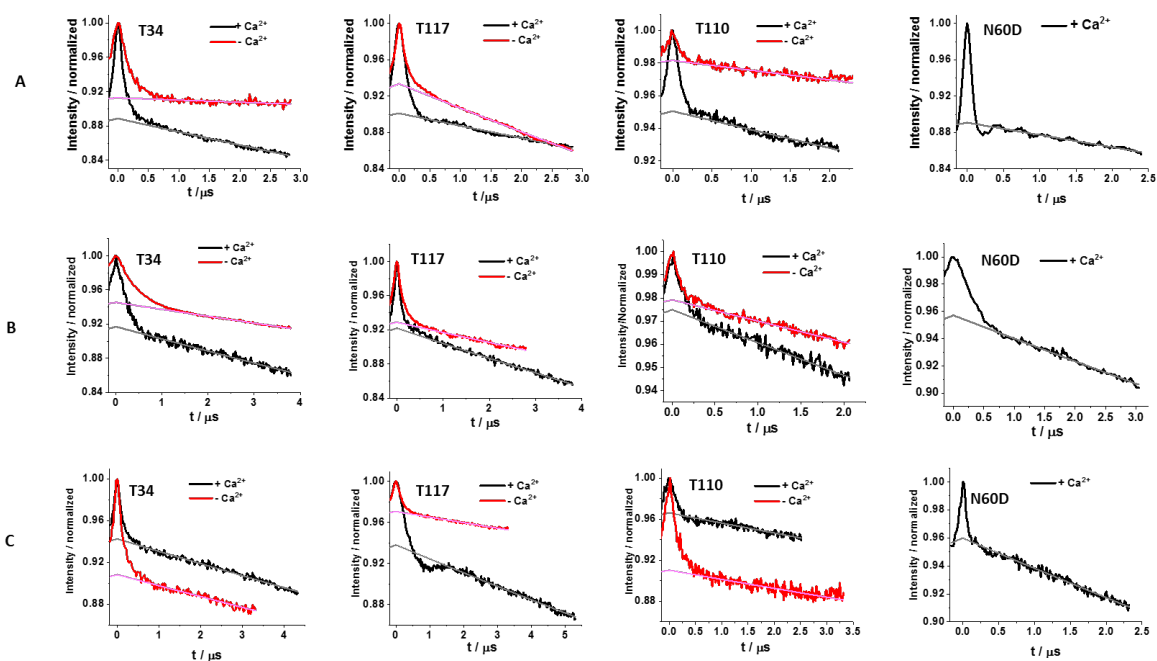


**Figure S11.** Primary DEER traces of the four CaM single mutants in the absence (red) or presence (black) of calcium together with background fits in grey and pink respectively. Panels A–C show the data obtained in the presence of the MARCKS, C-IQ and N-IQ peptide, respectively.

## 11. EPR spectra of MTSL-labelled IQ peptide with CaM

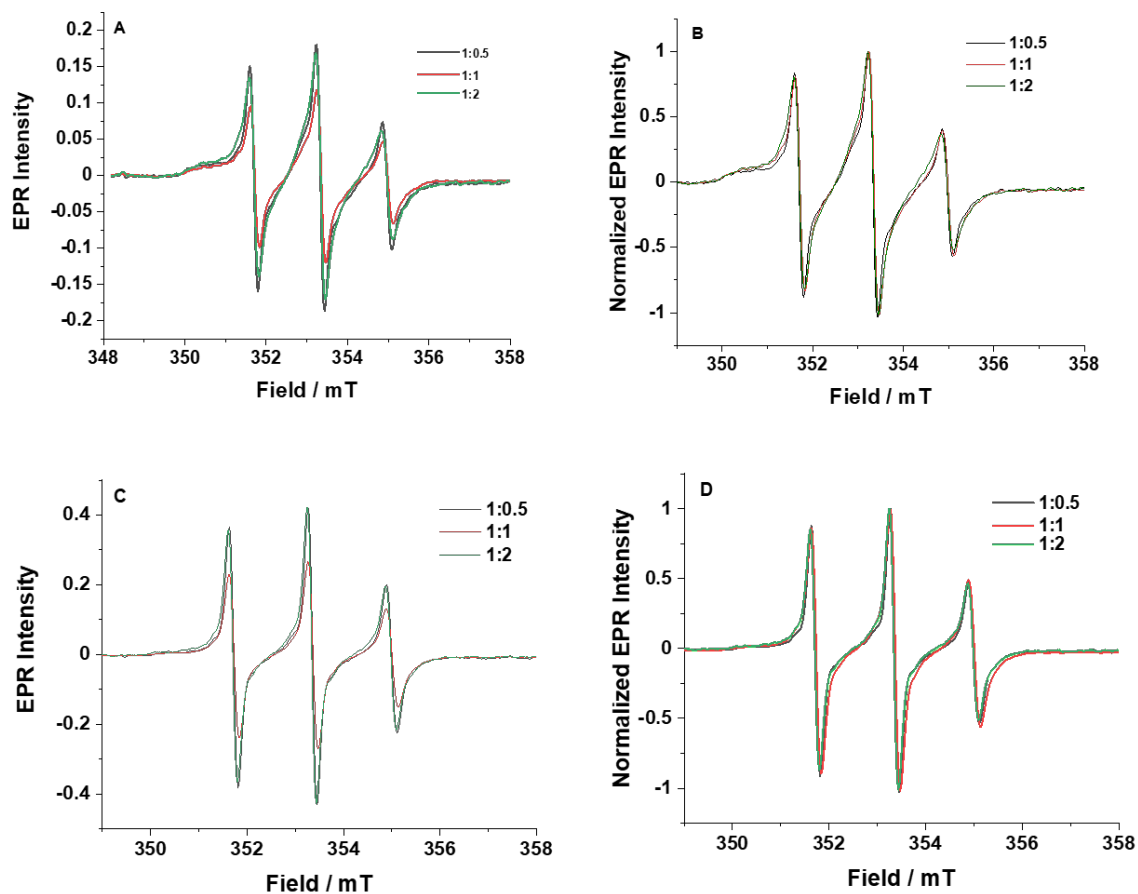


**Figure S12.** Room temperature X-band CW EPR measurements of C-IQ (50  $\mu$ M) binding to CaM. (A) Titration with increasing amounts of the CaM mutant T117C (molar ratio indicated in the figure) carried out in the absence of calcium (with EDTA present). (B) Same as (A), but following normalization of the spectra to the same maximum height. (C) and (D) Same as (A) and (B) but in the presence of 5 mM calcium .

## 12. Predicted vs experimental distance distributions in the CaM/IQ complex

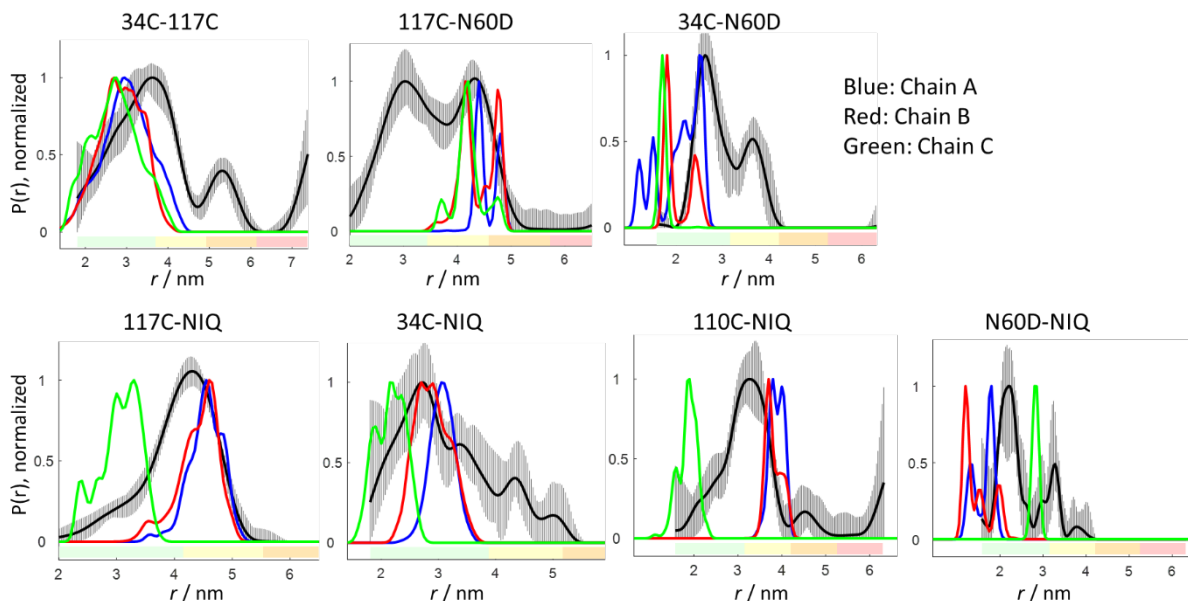


**Figure S13.** Comparison of the experimental distance distributions (Fig. 3 and Fig. 5) with those predicted for the three chains in the crystal structure 2BE6, as noted in the figure. The comparison with the A chain is shown in Figs. 3 and 5 in the main text. In the case of chains B and C, the crystal structure shows no electron density for the region labelled in the C-IQ peptide.

## 13. DEER data of doubly labelled IQ with CaM

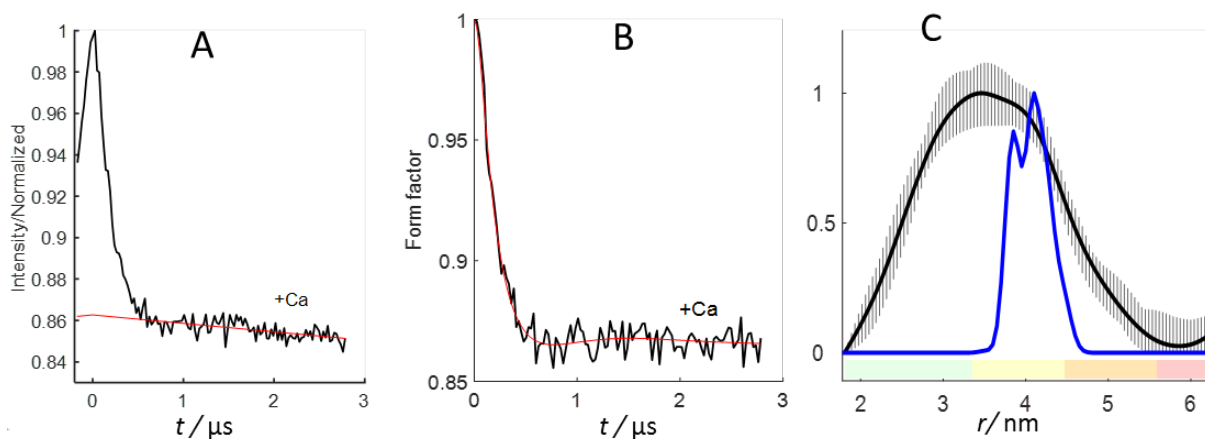


**Figure S14.** NO-NO DEER traces for unlabelled *holo*-CaM in the presence of IQ peptide labelled simultaneously in its N- and C-terminal segments. (A) Primary data (black line) with the background decay fit (red line) (B) Data after the removal of the background decay (black line) with the Tikhonov fit (red line), respectively. (C) Corresponding distance distribution. The blue line represents the predicted distance distribution from the crystal structure 2BE6, chain A, calculated using the program MMM.

#### 14. NMR data

**Table S2.** PCSs measured for backbone amide protons of CaM N60D in complex with MARCKS peptide in the presence of Tb(III) or Tm(III).

Residue	Tb(III)	Tm(III)
Thr5	0.83	-0.72
Glu6	1.06	-0.64
Glu7	1.13	-0.69
Glu11	1.13	-0.70
Lys13		-1.03
Leu18	0.60	
Gly23	0.60	-0.79
Thr34		1.43
Met36	-2.62	2.00
Asn42	-1.05	0.83
Glu45		0.61
Ala46		0.51
Glu47		1.16
Leu48		1.86
Arg90	-0.37	0.18
Val91	-0.18	0.08
Gly96	-0.17	0.08
Gly98	-0.13	0.10
Ile100	-0.15	0.09
Ser101	-0.14	0.09
Ala102	-0.14	0.10
Ala103	-0.16	0.11
Thr117	-0.02	0.02
Asp118	-0.04	0.02
Val121	-0.01	
Met124	-0.09	0.07
Ile130	-0.10	0.06
Asp131	-0.08	0.15
Asp133	-0.08	0.05
Gly134	-0.09	0.03
Gln135	-0.09	0.06
Val136	-0.18	0.13
Asn137	-0.11	0.12
Gln143	-0.20	0.06

**Table S3.**  $\Delta\chi$ -tensor parameters determined for CaM N60D in complex with MARCKS peptide calculated from N-domain PCSs.<sup>a</sup>

	Tb(III)	Tm(III)
$\Delta\chi_{ax}/10^{-32} \text{ m}^3$	54.0 (5.4)	27.5 (9.1)
$\Delta\chi_{rh}/10^{-32} \text{ m}^3$	12.6 (6.9)	11.0 (4.7)
$\alpha/^\circ$	14 (2)	87 (5)
$\beta/^\circ$	111 (2)	36 (14)
$\gamma/^\circ$	38 (6)	41 (8)
$Q$	0.03	0.09

<sup>a</sup> The  $\Delta\chi$ -tensor fits used the crystal structure 1IWQ and the metal position was constrained to the coordinates  $x = -9.645$ ,  $y = 22.186$  and  $z = 89.373$  (calcium-binding site II). The table displays the best fits. Standard deviations (in brackets) were determined from fits obtained by using the same metal position while randomly omitting 20% of the PCS data. Quality factors ( $Q$ ) were calculated as the root mean square (r.m.s.) of the differences between experimental and back-calculated PCSs divided by the r.m.s. of the experimental PCSs.

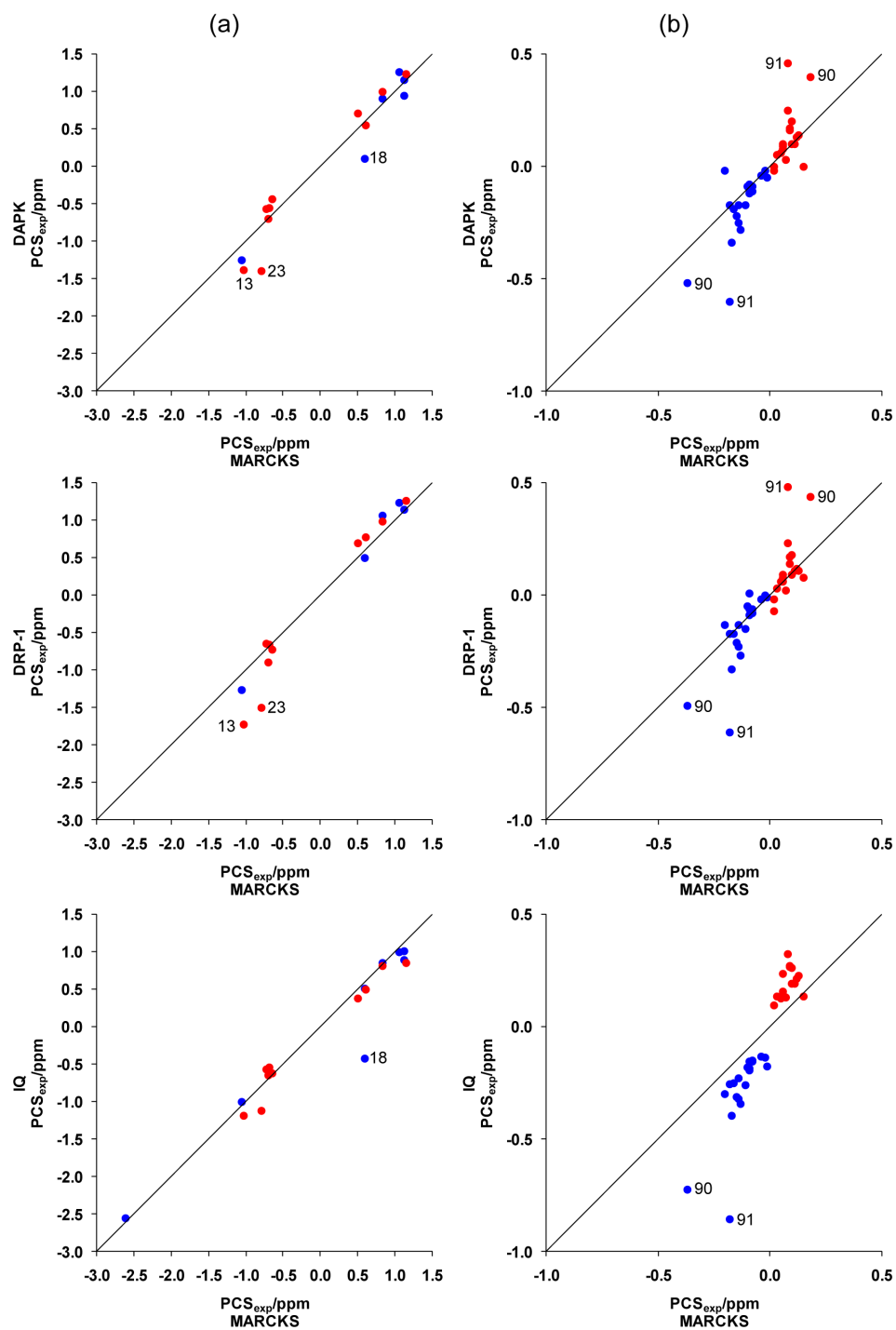


**Figure S15.** Correlation between experimental PCSs of the CaM-MARCKS complex and other globular CaM-target peptide complexes. (a) Correlations for N-domain residues. Blue and red points mark the PCSs obtained with Tb(III) and Tm(III), respectively. (b) Same as (a) but for the C-domain residues. Points with the largest deviations are marked with the corresponding residue number.

## 15. Restraints for the elastic network modelling and results

**Table S4.** List of restraints giving the maxima of the distance distributions (in nm) and their standard deviations, assuming Gaussian distributions.

Pair	Short		Average		Long	
	Max	SD	Max	SD	Max	SD
N-IQ-MTSL:C-IQ-MTSL	3.46	1.1	3.46	1.1	3.46	1.1
T34C-Gd-DOTA-M: T117-Gd-DOT-_M	3.64	0.8	3.64	0.8	3.64	0.8
N-IQ-MTSL/T34C-Gd-DOTA-M	2.7	0.8	2.7	0.8	2.7	0.8
N-IQ-MTSL/T110C-Gd-DOTA-M	3.31	0.6	3.31	0.6	3.31	0.6
N-IQ-MTSL/T117C-Gd-DOTA-M	4.31	0.5	4.31	0.5	4.31	0.5
C-IQ-MTSL/T34C-Gd-DOTA-M	3.77	0.6	3.77	0.6	3.77	0.6
C-IQ-MTSL/T110C-Gd-DOTA-M	3.36	1.0	3.36	1.0	3.36	1.0
C-IQ-MTSL/T117C-Gd-DOTA-M	2.62	0.7	2.62	0.7	2.62	0.7
N60D-Gd:T34C- MA-proxyl	3.02	0.7	3.58	0.94	4.32	0.5
N60D-Gd:T117C-MA-proxyl	2.48	0.5	2.48	0.5	2.48	0.5
N-IQ-MTSL/N60D-Gd	2.2	0.35	2.2	0.35	2.2	0.35
C-IQ-MTSL/N60D-Gd	4.23	0.6	4.23	0.6	4.23	0.6

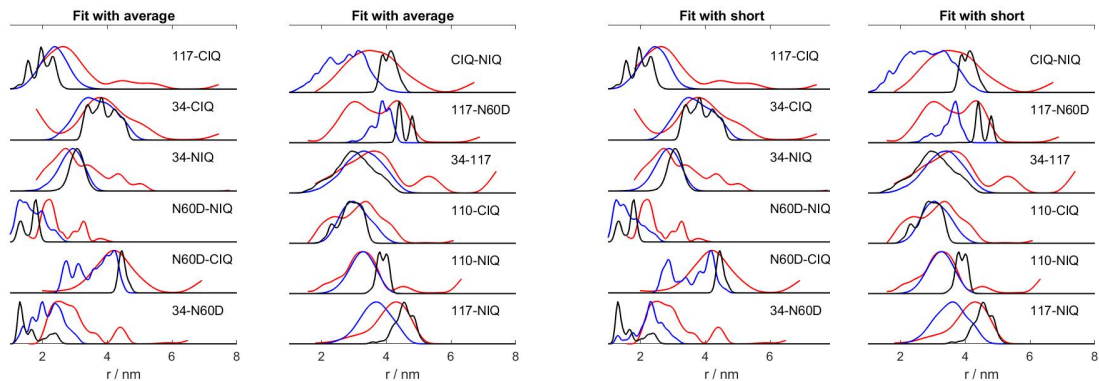


**Figure S16.** Comparison of the distance distributions obtained from fitting structures with the MMM software (blue) modelled with the average and short restraint options for *holo*-CaM N60D-Gd(III)/T117C-MA-proxy as indicated, predictions from the X-ray structure (black) and the experimental results (red) for all constructs of *holo*-CaM. Both options yield similar results.

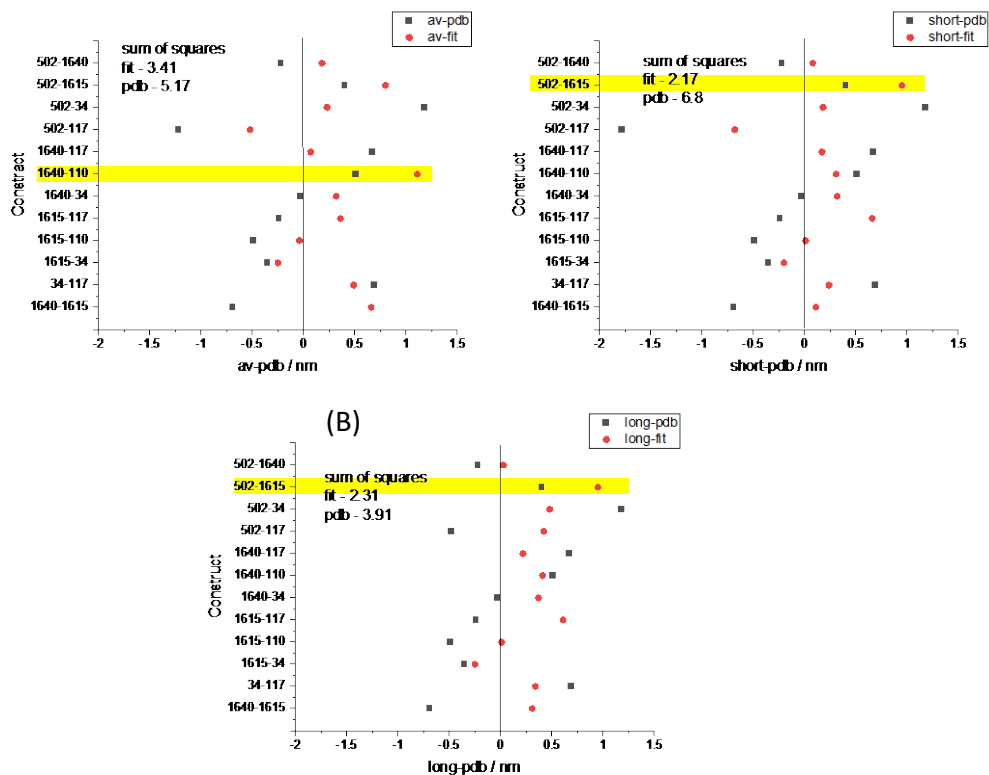


**Figure S17.** Deviation of the maxima of the distance distributions of the fitted structures from the experimental ones as compared to that of the X-ray structure (chanin A) and the experimental results obtained with with the restraints set as (A) average, (B) short and (C) long distances. Each panel also indicates the sum of squares of the differences in nm. The yellow bars highlight the construct with the largest deviation from the experimental result.

## 16. SDS gel

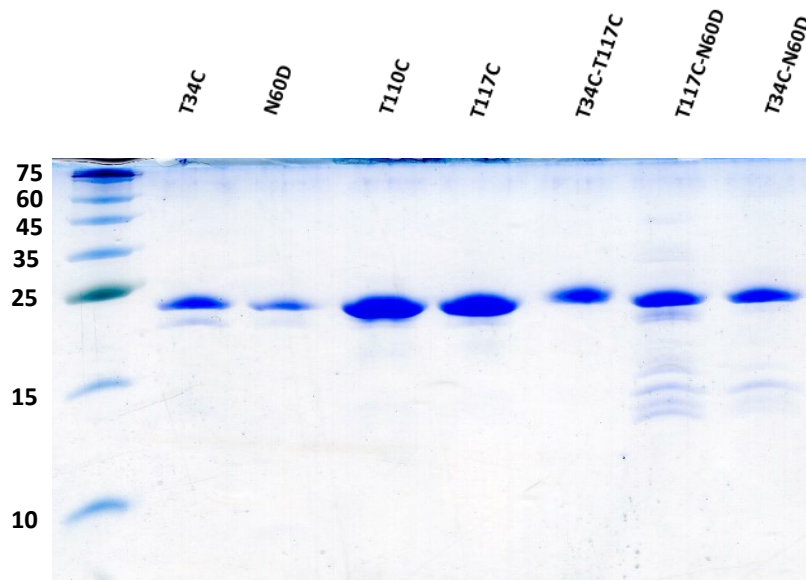


**Figure S18.** SDS-PAGE (16%) gel electrophoresis of CaM mutants. The band at about 20 kDa corresponds to the pure protein.